

SUPPLEMENTARY INFORMATION

Contribution of eigenmobility shifts to the separation of peptides in capillary electrophoresis with aqueous-acetonitrile background electrolytes.

Authors: Chadin Kulsing, Reinhard I. Boysen and Milton T. W. Hearn*

Australian Centre for Research on Separation Science (ACROSS), Centre for Green Chemistry, School of Chemistry, Monash University, Melbourne, Victoria 3800, Australia.

* Corresponding author: Prof. Milton T. W. Hearn

Phone: +61 3 9905 4547

E-mail address: milton.hearn@monash.edu

THEORY AND COMPUTATIONAL PROCEDURES

CALCULATION OF PEPTIDE pK_a

Physicochemical information for the peptides **1-5** is shown in **Table S1**. The pI and charge values, at pH 2.98 and 6.80, were calculated using the Hephaestus software developed at the Centre for Green Chemistry, Monash University and formatted as Microsoft Excel Professional Edition 2003 files.¹

SIMULATIONS WITH THE PROGRAM *PEAKMASTER*

The computer simulation program *Peakmaster* ver 5.2,² freely available at (<http://web.natur.cuni.cz/gas/>) was used to simulate the electro-chromatographs involving UV detection procedures. This software was adapted in house for use with other modes of detection, such as the ion current intensities at a specific m/z values signals generated by mass spectrometry.^{2,3}

Table S1. Amino acid sequences of the peptides **1-5** with their molecular masses, calculated pI values and charge at pH 3 and 7; with the pK_a values of these 5 peptides approximated to their pI values for incorporation as data entries into the *Peakmaster* software.

Peptide code	Sequence	Molecular mass	pI	Calculated charge at pH	
				2.98	6.80
1	Asp-Arg-Val-Tyr-Ile-His-Pro-Phe	1046.2	7.32	2.52	0.13
2	Val-Tyr-Val	379.5	5.70	0.62	-0.04
3	Gly-Tyr	238.2	5.70	0.62	-0.04
4	Tyr-Gly-Gly-Phe-Leu	555.6	5.45	0.62	-0.11
5	Tyr-Gly-Gly-Phe-Met	573.7	5.45	0.62	-0.11

The general input parameters employed with the *Peakmaster* software were 80 cm for the total length of the capillary to the detector, positive polarity at the injection site, 20 kV of driving voltage and the ionic strength correction turned on. The other input parameters utilised with the *Peakmaster* software were the concentrations, limiting mobilities and pK_a values of each BGE constituent and all analytes. The concentration of ammonium ions, fixed at 20.0 mM (with the $pK_a = 9.25$ and limiting mobility $= 76.2 \times 10^{-9} \text{ m}^2 \text{ v}^{-1} \text{ s}^{-1}$ taken from data in *Peakmaster*), and a concentration of 130.8 mM formic acid (with a $pK_a = 3.75$ and limiting mobility $= 56.6 \times 10^{-9} \text{ m}^2 \text{ v}^{-1} \text{ s}^{-1}$), and denoted by $[\text{NH}_4^+]$ and $[\text{HCOOH}]$, respectively, were put into *Peakmaster* at the measured pH 2.98 and $[\text{NH}_4^+] = 20.0 \text{ mM}$ ammonium ions and $[\text{HCOOH}] = 19.9 \text{ mM}$ formic acid at the measured pH 7.05. For example, when $[\text{HCOOH}] = 130.8 \text{ mM}$ was the formic acid concentration, the calculated pH value was the same as the measured, namely pH 2.98 with 0% acetonitrile. The same NH_4^+ ion concentration and the $[\text{HCOOH}]$ concentrations were the same in all experiments, with the amounts of all samples in the program being designated with an “S” (small values of the concentration).

Five peptides, **1-5**, were selected for determination of the positions of the suppression zones. Their pI values are shown in Table S1. The pK_a values, which were approximated to be the pI values of the peptides, were kept constant for each percentage of acetonitrile added, since the focus in this work -- the eigenmobility -- is not affected by the pK_a values of the sample.^{4,5} The limiting mobility values of each sample containing an organic solvent,⁶ were varied by iterative regression procedures until the simulated electropherograms matched the experimentally obtained mass electropherograms.

When a certain amount of acetonitrile is added, the relative permittivity and viscosity are changed, to higher and lower values, respectively, leading to variations in the activity coefficients of the buffer electrolyte (BGE) constituents. This effect was considered since an ionic strength correction was required for the simulations. Thus, all concentration profiles were replaced by their activity a_i ⁷ which is expressed by

$$a_i = \gamma_i c_i \quad (\text{Eqn S1}),$$

where c_i is the concentration of constituent i and γ_i is the activity coefficient which can be related to the ionic strength I with the relative charge z_i via the Debye-Hückel equation

$$\log \gamma_i = - \frac{A z_i^2 \sqrt{I}}{1 + B a_i \sqrt{I}}. \quad (\text{Eqn S2}).$$

The constants A and B are dependent on the relative permittivity and viscosity.⁶ Consequently, with aqueous BGEs containing acetonitrile, even though the value of the shifted pK_a and mobility are known, ionic strength corrections will result in a simulation that

fits the experimental results only when the value of A and B are known. Instead of determining the exact values of these constants, the constants A and B for an aqueous BGE without acetonitrile present were used as the default values in *Peakmaster*, with the resulting trends shown experimentally. The shift in the eigenmobility thus relates to the difference in the values between the calculated pH (after correction of the pK_a) and the measured pH of a given BGE at various percentages of acetonitrile.

CALCULATION OF THE pK_a SHIFT AFTER ADDITION OF ACETONITRILE TO A BGE

Upon addition of acetonitrile to the BGE, the pK_a and limiting mobility values of all constituents are changed.⁸ However, only the values for the NH_4^+ ion and HCOOH concentrations affect the parameter of interest, the eigenmobility. The change of pK_a values at any percentages of acetonitrile, in case of the neutral acid (HA), can be expressed as:⁹

$$pK_{a, \text{ in water }} - pK_{a, \text{ in mixture }} = \Delta pK_a = \log \gamma_{H^+}^m + \log \gamma_{A^-}^m - \log \gamma_{HA}^m \quad (\text{Eqn S3}),$$

where $\gamma_{H^+}^m$, $\gamma_{A^-}^m$ and γ_{HA}^m are the transfer activity coefficients for the ionization equilibrium of protonated, anionic and neutral molecules,⁹ respectively. Eqn S3 reflects mainly the differences in solvation energy of each constituent before and after the addition of acetonitrile.^{10,11} In practice, the pK_a -shift in acetonitrile can be expressed as¹²

$${}_S pK_a = a_S {}^W pK_a + b_S + \delta \quad (\text{Eqn S4}),$$

where ${}_S pK_a$ is the pK_a value measured in an acetonitrile/aqueous BGE mixture and calibrated against pure water as the default solvent, ${}^W pK_a$ is the pK_a value measured with a BGE at 0% acetonitrile which is also calibrated against pure water and can be calculated from knowledge of the fitting constants a_s and b_s : given by Eqns. S5 and S6, respectively:

$$a_S = \frac{1 + a_{S1} \phi_{ACN} + a_{S2} \phi_{ACN}^2}{1 + a_{S3} \phi_{ACN} + a_{S4} \phi_{ACN}^2} \quad (\text{Eqn S5})$$

$$\text{and } b_S = \frac{b_{S1} \phi_{ACN} + b_{S2} \phi_{ACN}^2}{1 + b_{S3} \phi_{ACN} + b_{S4} \phi_{ACN}^2} \quad (\text{Eqn S6}),$$

where ϕ_{ACN} is the volume fraction of acetonitrile in the mixture and $a_{S1}, a_{S2}, a_{S3}, a_{S4}, b_{S1}, b_{S2}, b_{S3}$ and b_{S4} are fitting constants derived from literature examples¹² and specific to the types of sample, e.g., aliphatic carboxylic acids, amines, etc.

Based on the above approach, the ${}_S pK_a$ values of both the NH_4^+ ions and HCOOH at pH 2.98 for different percentages of acetonitrile were calculated and the results are shown in the range 0% to 50% (v/v) acetonitrile in Table S2.

Table S2. Calculated ${}^S_w pK_a$ values of the NH_4^+ and HCOOH at pH 2.98 containing different percentages of acetonitrile required as input values into *Peakmaster*.

Species	${}^S_w pK_a$ at various % (v/v) acetonitrile										
	0	5	10	15	20	25	30	35	40	45	50
HCOOH	3.752	3.896	4.006	4.105	4.202	4.300	4.403	4.512	4.630	4.758	4.900
NH_4^+	9.250	9.220	9.180	9.132	9.075	9.008	8.932	8.848	8.757	8.664	8.571

MOBILITY SHIFTS AFTER ADDITION OF ACETONITRILE TO THE BGE

When an amount of acetonitrile is added to a BGE, besides the pK_a change, the relative permittivity and viscosity will also change and these variations will affect the mobility of the ion of interest. This effect can be accommodated, according to the Debye-Hückel-Onsager limiting approach, by including the contribution of ion size of mean diameter a in Ångstroms, which leads to the following relationship, Eqn. S7, between the ion mobility and the relative permittivity of the BGE ¹¹:

$$\mu_i = \mu_{0,i} - \left[\frac{8.204 \times 10^5}{(\epsilon T)^{3/2}} \mu_{0,i} + \frac{42.75}{\eta (\epsilon T)^{1/2}} \right] \cdot \frac{\sqrt{I}}{1 + 50.29 a (\epsilon T)^{-1/2} \sqrt{I}} \quad (\text{Eqn S7}),$$

where ϵ is the relative permittivity, η is the viscosity (in Poise), I is the ionic strength (M) and T (K) is the absolute temperature. This equation illustrates that the ion mobility, $\mu_i (10^{-9} \text{m}^2 \text{V}^{-1} \text{s}^{-1})$, will increase towards its limiting value, $\mu_{0,i}$, as the relative permittivity increases. One parameter that is difficult to assess is the limiting value of the ion diameter, which can vary at different percentages of acetonitrile and, sometimes, can be higher in aquo-organic solvent mixtures than that in pure water. The limiting value of the ion mobility can be obtained by extrapolating the plot of mobility *versus* $\frac{\sqrt{I}}{1 + 50.29 a (\epsilon T)^{-1/2} \sqrt{I}}$. ^{6,11} However, these values need to be calculated for each studied BGE. Since determination of the absolute peptide mobility values was not the aim in this study, the simulations employed in this investigation were based on iterative procedures with the relative limiting mobility value of each peptide adjusted until the simulation fitted to the experimental chromatograms.

THE EFFECT OF RADIAL DISTRIBUTION

The distribution of a target species in a cylindrical capillary under the influence of an electric field can be evaluated from the Poisson-Boltzmann equation as extended by the

Debye-Hückel approximation, assuming that a radial symmetry occurs, according to Eqns S8 and S9:

$$\rho_{DH}(r) = \zeta \varepsilon_0 \varepsilon_r \kappa^2 \frac{I_0(\kappa r)}{I_0(\kappa R)} \quad (\text{Eqn S8})$$

$$u_{DH}(r) = \frac{\zeta \varepsilon_0 \varepsilon_r E_z}{\eta} \left[1 - \frac{I_0(\kappa r)}{I_0(\kappa R)} \right] \quad (\text{Eqn S9}),$$

where r is the radial coordinate in a cylinder having the radius R (in units of the Debye-Hückel length, κ), $\rho_{DH}(r)$ and $u_{DH}(r)$ are the charge density and mobility at r assuming the Debye-Hückel approximation prevails, k is the Boltzmann constant ($=1.38 \times 10^{-23} \text{ JK}^{-1}$), ε_0 is the permittivity of vacuum ($=8.854 \times 10^{-12} \text{ C}^2 \text{ J}^{-1}$), ε_r is the relative permittivity, κ^{-1} is defined as the double layer thickness, ζ is the zeta-potential (v), η is the viscosity, E_z is the applied voltage (v m^{-1}) and I_0 is the zero-order modified Bessel function of the first kind.

The benefits of these equations allow the amount of the target constituent (any species containing a non-zero charge) to be evaluated at the distance r from the surface of the inner wall of a capillary. In our case, the magnitude of the radial distribution due to the electric field experienced by the target constituent was considered, since this is caused by the double layer, leading to the EOF, and the tube radial distribution of the aqueous-acetonitrile system within the capillary.¹³⁻¹⁵

In addition to a continuous radial distribution of the constituents, two discontinuous regions within the capillary also need to be considered where differences in ion mobilities can be experienced, namely the region proximal to the inner wall of the capillary and the region associated with the lumen (*i.e.* at the centre) of the capillary. Due to participation of the double layer effect, ion mobility within the double layer will be lower than that at the centre of the capillary, and in fact will become zero at the electro-stagnant 0th plane layer of the double layer. These two regions are expected to cause a single constituent to behave like two constituents moving with two different mobilities and pK_a values. The behaviour of this ‘virtual’ 4-constituent BGE (assuming that 2 constituents can be assigned to the inner wall and the lumen regions) was then simulated using the *Peakmaster* software.

CALCULATION OF NH_4^+ ION CONCENTRATION VALUES AT THE INNER WALL SURFACE OF THE CAPILLARY AND IN THE BULK BGE AS A RESULT OF THE DOUBLE LAYER EFFECT AND PLOTTED AS SHOWN IN FIGURE 3B

From the Eqn S7, the electro-osmotic flow in the middle of the capillary at $r = 0$, can be approximated by:

$$\mu_{EO} = \mu_{DH}(0) = \frac{\zeta \varepsilon_0 \varepsilon_r E_z}{\eta} \left[1 - \frac{I_0(0)}{I_0(\kappa R)} \right] \approx \frac{\zeta \varepsilon_0 \varepsilon_r E_z}{\eta}, R \gg \kappa \quad (\text{Eqn S10}),$$

where μ_{EO} is the electroosmotic flow mobility (EOF mobility, $\text{m}^2\text{v}^{-1}\text{s}^{-1}$). By using the Boltzmann distribution between the NH_4^+ ions at the capillary wall surface and in the bulk region, the value of the $[\text{NH}_4^+]_0$, *i.e.* the concentration of NH_4^+ ions at the inner wall surface of the capillary, $\rho_{DH}(R)$, can be calculated as ¹⁶

$$\log \frac{[\text{NH}_4^+]_0}{[\text{NH}_4^+]} = Y(T) \mu_{EO} \quad (\text{Eqn S11}).$$

For a BGE without acetonitrile present, $\rho_{DH,0\%}(R) = [\text{NH}_4^+]_0 = 20 \times 10^{0.2169\mu_{EO}}$, and $Y(T) = \frac{528.67 \exp(\frac{1958}{T} + 0.004605T)}{\ln(10)T} = 0.2169 \text{ v s m}^{-2}$, at $T = 298 \text{ K}$,¹⁶ for all the studied BGEs, $[\text{NH}_4^+] = 20 \text{ mM}$. In the case of a BGE containing acetonitrile, from the Eqn S8 at the capillary wall surface, $I_0(\kappa r) = I_0(\kappa R)$, then

$$\rho_{DH}(R) = \zeta \varepsilon_0 \varepsilon_r \kappa^2 \quad (\text{Eqn S12})$$

$$\frac{\rho_{DH,0\%}(R)}{\rho_{DH,a\%}(R)} = \frac{\zeta_{0\%} \varepsilon_{r,0\%} \kappa_{0\%}^2}{\zeta_{a\%} \varepsilon_{r,a\%} \kappa_{a\%}^2} \quad (\text{Eqn S13})$$

where the subscripts, $a\%$, indicate the parameter at a percentage of acetonitrile (v/v) in the BGE (0% being the BGE without addition of acetonitrile) and $\kappa^2 = \frac{2e^2 I}{\varepsilon_0 \varepsilon_r kT}$. Substitution of this term into the Eqn S13, assuming that I remains constant along the capillary, yields

$$\frac{\rho_{DH,0\%}(R)}{\rho_{DH,a\%}(R)} = \frac{\zeta_{0\%}}{\zeta_{a\%}} = \frac{\mu_{EO,0\%} \eta_{0\%} / \varepsilon_{r,0\%}}{\mu_{EO,a\%} \eta_{a\%} / \varepsilon_{r,a\%}} \quad (\text{Eqn S14})$$

or

$$\rho_{DH,a\%}(R) = \frac{\mu_{EO,a\%} \eta_{a\%} / \varepsilon_{r,a\%}}{\mu_{EO,0\%} \eta_{0\%} / \varepsilon_{r,0\%}} \rho_{DH,0\%}(R) \quad (\text{Eqn 15}).$$

Using literature values of the η and ζ for aqueous/acetonitrile mixtures,^{17,18} the values of $\frac{\eta_{a\%} / \varepsilon_{r,a\%}}{\eta_{0\%} / \varepsilon_{r,0\%}}$ for BGEs containing different percentages of acetonitrile were calculated (using also the literature value of the ε_r ^{17,18}). In this manner, it was possible to calculate the $[\text{NH}_4^+]_0$ ion concentrations at different percentages of acetonitrile from the EOF values.

APPROXIMATION OF NH_4^+ ION CONCENTRATION VALUES AT THE INNER WALL SURFACE AND IN THE CENTRE (LUMEN) OF THE CAPILLARY AS A RESULT OF TUBE RADIAL DISTRIBUTION FOR AN AQUEOUS-ACETONITRILE SYSTEM IN CE AS PLOTTED IN FIGURE 3C

Under the influence of the electrical driving force, an aqueous BGE containing less than 50% (v/v) of acetonitrile (bulk concentration) is expected to behave like a biphasic system with a water-rich phase in the centre of the capillary, and an acetonitrile-rich phase at or close to the double layer within the capillary, denoted by WRP and ARP, respectively. Regardless of the effect of the electric field in the z-direction (along the length of the capillary), the distribution of the NH_4^+ ions in the WRP and the ARP phase, *i.e.* $[\text{NH}_4^+]_W$ and $[\text{NH}_4^+]_A$, respectively, will occur as a result of potential energy differences which arise due to the effects of different ionic atmospheres, as illustrated by using the Boltzmann distribution. From the Poisson-Boltzmann equation and by using a Debye-Hückel approximation with a first order Taylor series expansion for the exponential term,¹⁹ the potential energy U of such BGE solution mixtures can be given by

$$U = -\frac{q^2\kappa}{4\pi\epsilon_0\epsilon_r}\sum_i^s \frac{c_i z_i^2}{2(1+\kappa a_i)} \quad (\text{Eqn S16}).$$

If a Boltzmann distribution prevails, then the ratio of NH_4^+ ion concentrations in each BGE phase can be estimated from:

$$\frac{[\text{NH}_4^+]_W}{[\text{NH}_4^+]_A} = e^{\frac{-\Delta U}{kT}} \quad (\text{Eqn S17}),$$

where ΔU is the potential energy difference between the WRP and the ARP and

$$\Delta U = U_W - U_A = -\frac{q^2\kappa_W}{4\pi\epsilon_0\epsilon_{r,W}}\sum_i^s \left[\frac{c_i z_i^2}{2(1+\kappa_W a_{i,W})} \right] + \frac{q^2\kappa_A}{4\pi\epsilon_0\epsilon_{r,A}}\sum_i^s \left[\frac{c_i z_i^2}{2(1+\kappa_A a_{i,A})} \right] \quad (\text{Eqn S18}).$$

The sign of ΔU is of importance since, after acetonitrile is added, it indicates that the BGE phase contains a higher or lower NH_4^+ ion concentration. For example, from the Eqn S17, when $\Delta U > 0$, the term $e^{\frac{-\Delta U}{kT}}$ is less than one which means that a higher NH_4^+ ion concentration is found in the ARP. On the other hand, when $\Delta U < 0$, a higher NH_4^+ ion concentration will occur in the WRP. The NH_4^+ ion concentration in both BGE phases is the same when $\Delta U = 0$.

If it is assumed that the ionic strength in both BGE phases is the same, the activity coefficients of all constituents are 1 in both BGE phases, all constituents share the same value of $a_{i,W}$ and $a_{i,A}$ $\left(\sum_i^s \left[\frac{c_i z_i^2}{2(1+\kappa_W a_{i,W})} \right] = \frac{I}{(1+\kappa_W a_{i,W})} \right)$, and both BGE phase zones essentially operate independently with a fixed percentage, say 0%, acetonitrile in the water-rich phase and any percentage of acetonitrile in the acetonitrile-rich phase, then the Eqn S18 can be rearranged into

$$\Delta U = U_W - U_A = \frac{z^2 e^3 I^{3/2}}{2^{3/2} \pi (kT)^{1/2} \epsilon_0^{3/2}} \left[-\frac{1}{\epsilon_{r,W}^{3/2} (1 + \kappa_W a_{i,W})} + \frac{1}{\epsilon_{r,A}^{3/2} (1 + \kappa_A a_{i,A})} \right] \quad (\text{Eqn S19}).$$

Since, I is assumed to be constant, the term $\frac{z^2 e^3 I^{3/2}}{2^{3/2} \pi (kT)^{1/2} \epsilon_0^{3/2}}$ becomes constant for all possible percentages of acetonitrile. In this case, to determine the sign of ΔU , the values of κ , the static ϵ_r (the value at zero frequency) and a_i in both BGE phases were taken from reference²⁰ and in our case $I = 20.929$ mM (the calculated value from the *Peakmaster* without ionic strength correction, with the input [ammonium] = 20 mM and [formic acid] = 130.8 mM). The term in parenthesis in Eqn S16 can be defined as M_P . The calculated values of M_P at different percentages of acetonitrile in the ARP are shown in Table S3.

Table S3. Calculated values of $[\text{NH}_4^+]_{\text{ARP}}$ and the parameters involved, at a fixed $[\text{NH}_4^+]_{\text{WRP}} = 20$ mM at $T = 298$ K, for BGEs containing differing percentages of acetonitrile in the Acetonitrile Rich Phase.

%v/v ACN in ARP	ϵ_r ^a	M_P ^b	ΔU ^c / J	$[\text{NH}_4^+]_{\text{ARP}}$ / mM
0	78.36	-	-	-
10	74.92	0.0001	0.050	21.03
20	70.49	0.0002	0.124	22.63
30	65.57	0.0004	0.220	24.92
40	60.61	0.0007	0.337	28.03
50	55.69	0.0010	0.480	32.33
60	51.05	0.0013	0.647	38.21
70	46.83	0.0017	0.830	46.14
80	43.10	0.0021	1.042	56.69
90	39.41	0.0026	1.295	73.00
100	35.88	0.0032	1.599	98.95

^a Values from reference [19].

$$\supset M_P = -\frac{1}{\epsilon_{r,W}^{3/2} (1 + \kappa_W a_{i,W})} + \frac{1}{\epsilon_{r,A}^{3/2} (1 + \kappa_A a_{i,A})}$$

$$\supset \Delta U = U_W - U_A$$

Regardless of the change in ionic strength at different amounts of acetonitrile, the sign of M_P is the same as that of ΔU . After adding acetonitrile to the aqueous BGE, all M_P values

become positive (more negative values of potential energies in the ARP) with the higher values corresponding to the higher percentages of acetonitrile in ARP.

From Equation S19, by taking the ratio of ΔU values at any two values of % (v/v) acetonitrile in ARP, $\Delta U_{A,a\%}$ and $\Delta U_{A,b\%}$, the following relationship can be derived

$$\frac{\Delta U_{A,a\%}}{\Delta U_{A,b\%}} = \frac{M_{p,a\%}}{M_{p,b\%}} \quad (\text{Eqn S20}),$$

where $M_{p,a\%}$ and $M_{p,b\%}$ are the values of M in the case of having an $a\%$ or a $b\%$ of acetonitrile (v/v) in the ARP, with that in the WRP at 0% acetonitrile.

Since an aim of this investigation was to illustrate that if phase separation occurs in the BGE containing a certain percentage of acetonitrile (whatever the driving force may be, *e.g.*, electrical, chemical potential difference or capillary pressure force), the acetonitrile added into the BGE will leads to a change in $[\text{NH}_4^+]_W / [\text{NH}_4^+]_A$. With $M_{p,b\%} = M_{p,10\%}$ as an example, the value of $\Delta U_{A,10\%} = 0.05 \text{ J}$. The values of $\Delta U_{A,a\%}$ at the other percentages of acetonitrile in ARP, as shown in Table S3, can be found from the Eqn. S20 and the corresponding $M_{p,a\%}$.

The derived values, calculated according to a Boltzmann distribution and Eqn. S16, of $[\text{NH}_4^+]_A$ by having $[\text{NH}_4^+]_W$ set at a constant value of 20 mM are shown in Table S3. The potential energy in the ARP is thus lower than that in the WRP, which means that higher amounts of acetonitrile in the BGE can lead to higher NH_4^+ ion concentrations in the ARP if the correction values of the ionic strength for BGEs with different percentages of acetonitrile do not vary significantly. These studies were intended to show that if NH_4^+ ions move to the outer layer ARP, and if phase separation occurred in a capillary at, say, 10% (v/v) acetonitrile in the ARP, the $[\text{NH}_4^+]_A$ could increase exponentially. This behaviour is based on the Boltzmann distribution. As the acetonitrile content is increased further, the $[\text{NH}_4^+]_A$ values at 100% (v/v) acetonitrile in the ARP could reach more than four times the value with 10% (v/v) acetonitrile in the ARP, see Table S3. These outcomes have strong implications on the separation behaviour of peptides or any other polar ionisable analytes in CE with aqueous-organic BGEs.

SIMPLIFICATION AND SIMULATION OF ION RADIAL DISTRIBUTION EFFECT ON THE EIGENMOBILITY CHANGE

To illustrate more clearly the effect of the radial distribution of BGE ions, caused by either the double layer formation or phase separation in the capillary, on the eigenmobility,

the more simplified case of a one dimensional scenario was considered. Simulation by the *Peakmaster* program considering only the significant influences on the eigenpeak mobility was then performed. Based on the fact that there is a higher amount of H^+ ions and NH_4^+ ions near to the wall surface of the capillary, the BGE constituents were separately treated as moving as two independent radial parts (or zones) of the capillary. In Figure S1, Zone 1, the BGE constituents are moving faster with lower pK_a value than that of HCOOH (representing the BGE constituent in the centre of the capillary) and Figure S1 Zone 2 represents the BGE constituents moving slower with a higher pK_a value than that of HCOOH (representing the constituent being near the wall surface of the capillary). The effect of the pK_a of the HCOOH in each phase on the eigenmobility at different percentages of acetonitrile can then be rationalised in the same way as that illustrated in Figure 2, except that only the effect of each part or zone of NH_4^+ ion concentration on the eigenmobility shift with 0-25% (v/v) acetonitrile in the bulk BGE is considered.

For example, if the BGE constituents in Zone 1 and 2 have the limiting mobility of 76.2 and 30.0 $m^2v^{-1}s^{-1}$, respectively, by keeping the concentration of the NH_4^+ ions in the Zone 1 (in bulk), denoted by $[NH_4^+ \text{ in Zone 1}]$, in all studied BGEs at 20 mM, the concentrations of the NH_4^+ ions in the Zone 2, denoted by $[NH_4^+ \text{ Zone 2}]$, the simulated eigenmobility values can be calculated. The high degree of fit of these simulated data with the corresponding experimental values for a BGE containing 0 to 25% (v/v) acetonitrile in the bulk are shown in Figure 3C. It can be noted that the pK_a -values of HCOOH were varied so that the calculated and experimented pH values were the same for all studied BGE. This approach means that the pH shifts in all cases were already corrected without affecting the pK_a in the ARP. From Figure 3C it can be seen that the concentration of the NH_4^+ ions at the inner capillary surface layer was higher when ARP contained a higher percentage of acetonitrile. The reason could be that in a water rich carrier system, the ARP is pushed closer to the inner surface of the capillary.¹³ The percentage of acetonitrile in the ARP thus affects directly the NH_4^+ ion distribution close to the inner wall surface of the capillary. This effect can be explained in the same way as the EOF which was increased with BGEs containing higher percentages of acetonitrile, Table S4.

Increasing concentrations of NH_4^+ ions near to the inner surface of the capillary (calculated by using *Peakmaster*, Figure 3C) were required in order to achieve the experimental value of eigenmobility for BGEs containing 25% (v/v) acetonitrile as shown in Figure 3A. This increasing trend is in agreement with the profiles of the radial distribution

resulting from both EOF and phase separation calculated by using the Boltzmann distribution, Figures 3B and 3C. In other words, the nonlinearity shown in Figure 3A can be satisfactorily explained by the effect of radial distribution of the BGE ions in a capillary, when the pK_a , ionic strength and mobility corrections are included.

ADDITIONAL REFERENCES

- (1) Pesek, J. J.; Matyska, M. T.; Dawson, G. B.; Chen, J. I.; Boysen, R. I.; Hearn, M. T. W. *Anal. Chem.* **2004**, 76, 23-30.
- (2) Jaros, M.; Hruska, V.; Stedry, M.; Zuskova, I.; Gas, B. *Electrophoresis* **2004**, 25, 3080-3085.
- (3) Gas, B.; Hruska, V.; Dittmann, M.; Bek, F.; Witt, K. *J. Sep. Sci.* **2007**, 30, 1435-1445.
- (4) Stedry, M.; Jaros, M.; Gas, B. *J. Chromatogr. A* **2002**, 960, 187-198.
- (5) Stedry, M.; Jaros, M.; Vcelakova, K.; Gas, B. *Electrophoresis* **2003**, 24, 536-547.
- (6) Vcelakova, K.; Zuskova, I.; Porras, S. P.; Gas, B.; Kenndler, E. *Electrophoresis* **2005**, 26, 463-472.
- (7) Jaros, M.; Vcelakova, K.; Zuskova, I.; Gas, B. *Electrophoresis* **2002**, 23, 2667-2677.
- (8) Sarmini, K.; Kenndler, E. *J. Biochem. Biophys. Methods* **1999**, 38, 123-137.
- (9) Sarmini, K.; Kenndler, E. *J. Chromatogr., A* **1998**, 806, 325-335.
- (10) Sarmini, K.; Kenndler, E. *J. Chromatogr., A* **1999**, 833, 245-259.
- (11) Porras, S. P.; Riekkola, M. L.; Kenndler, E. *J. Chromatogr. A* **2001**, 924, 31-42.
- (12) Subirats, X.; Roses, M.; Bosch, E. *Sep. Purif. Rev.* **2007**, 36, 231-255.
- (13) Jinno, N.; Murakami, M.; Hashimoto, M.; Tsukagoshi, K. *Anal. Sci.* **2010**, 26, 737-742.
- (14) Murakami, M.; Jinno, N.; Hashimoto, M.; Tsukagoshi, K. *Chem. Lett.* **2010**, 39, 272-273.
- (15) Yamada, K.; Jinno, N.; Hashimoto, M.; Tsukagoshi, K. *Anal. Sci.* **2010**, 26, 507-510.
- (16) Vinther, A.; Soeberg, H. *J. Chromatogr.* **1992**, 589, 315-319.
- (17) Slusher, J. T. *Mol. Phys.* **2000**, 98, 287-293.
- (18) Helambe, S. N.; Lokhande, M. P.; Kumbharkhane, A. C.; Mehrotra, S. C.; Doraiswamy, S. *Pramana* **1995**, 44, 405-410.
- (19) Debye, P.; Huckel, E. *Phys. Z.* **1923**, 24, 185-206.
- (20) Gagliardi, L. G.; Castells, C. B.; Rafols, C.; Roses, M.; Bosch, E. *J. Chem. Eng. Data* **2007**, 52, 1103-1107.

FIGURES AND TABLES

Table S1. Amino acid sequences of five peptides with their molecular masses and calculated *pI* and charge at pH 3 and 7; the *pI* approximated to be the pK_a values of 5 samples in *Peakmaster*.

Peptide code	Sequence	Molecular mass	<i>pI</i>	Calculated charge at pH	
				2.98	6.80
1	Asp-Arg-Val-Tyr-Ile-His-Pro-Phe	1046.2	7.32	2.52	0.13
2	Val-Tyr-Val	379.5	5.70	0.62	-0.04
3	Gly-Tyr	238.2	5.70	0.62	-0.04
4	Tyr-Gly-Gly-Phe-Leu	555.6	5.45	0.62	-0.11
5	Tyr-Gly-Gly-Phe-Met	573.7	5.45	0.62	-0.11

Table S2. Calculated ${}_w^S pK_a$ values of the NH_4^+ and HCOOH at pH 2.98 containing different percentages of acetonitrile required as input values into *Peakmaster*.

Species	${}_w^S pK_a$ at various % acetonitrile (v/v)										
	0	5	10	15	20	25	30	35	40	45	50
HCOOH	3.752	3.896	4.006	4.105	4.202	4.300	4.403	4.512	4.630	4.758	4.900
NH_4^+	9.250	9.220	9.180	9.132	9.075	9.008	8.932	8.848	8.757	8.664	8.571

Table S3. Calculated values of $[\text{NH}_4^+]_{\text{ARP}}$ and the parameters involved, at a fixed $[\text{NH}_4^+]_{\text{WRP}} = 20 \text{ mM}$ at $T = 298 \text{ K}$, for BGEs containing differing percentages of acetonitrile in the Acetonitrile Rich Phase.

%v/v ACN in ARP	ϵ_r ^a	M ^b	ΔU ^c / J	$[\text{NH}_4^+]_{\text{ARP}}$ / mM
0	78.36	-	-	-
10	74.92	0.0001	0.050	21.03
20	70.49	0.0002	0.124	22.63
30	65.57	0.0004	0.220	24.92
40	60.61	0.0007	0.337	28.03
50	55.69	0.0010	0.480	32.33
60	51.05	0.0013	0.647	38.21
70	46.83	0.0017	0.830	46.14
80	43.10	0.0021	1.042	56.69
90	39.41	0.0026	1.295	73.00
100	35.88	0.0032	1.599	98.95

^a Values from reference²⁰.

$$^b M = -\frac{1}{\epsilon_{r,W}^{3/2}(1+\kappa_W a_{i,W})} + \frac{1}{\epsilon_{r,A}^{3/2}(1+\kappa_A a_{i,A})}$$

$$^c \Delta U = U_W - U_A$$

Table S4. The calculated (*Peakmaster*) and experimental values of eigenpeak mobility – EOF) and pH at different percentages of acetonitrile with the corresponding measured values of EOF; the experimental values of (eigenpeak mobility – EOF) at 0, 10, 20 and 25% (v/v) acetonitrile being close to those mobility of calculated at 0% acetonitrile, peptide **1** at 10% (v/v) acetonitrile, peptide **2** at 20% (v/v) acetonitrile and peptide **5** at 25% (v/v) acetonitrile, respectively, with the error bars indicated in Figure 3A.

%v/v ACN	EOF mobility ($10^{-9}\text{m}^2\text{v}^{-1}\text{s}^{-1}$)	Eigenpeak mobility - EOF ($10^{-9}\text{m}^2\text{v}^{-1}\text{s}^{-1}$)		pH	
		Calculated	Experimental	Calculated	Experimental
0	28.60	24.35	24.35	2.98	2.98
10	27.14	15.48	15.87	3.22	3.09
20	28.00	10.37	10.10	3.41	3.23
25	29.22	8.46	3.20	3.51	3.31
30	30.55	6.80	-	3.61	3.40
40	33.42	4.15	-	3.83	3.58
50	35.38	2.28	-	4.10	3.74
60	40.06	1.04	-	4.45	3.94

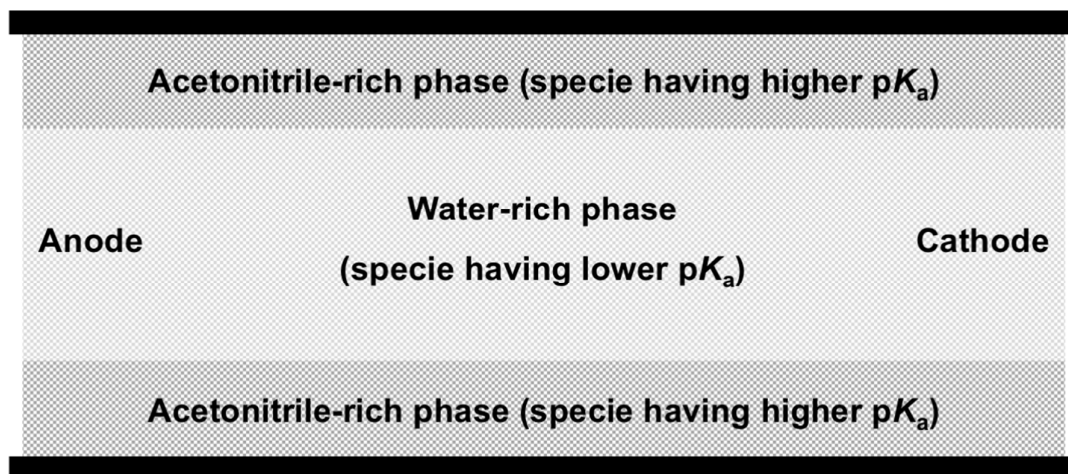


Figure S1. Schematic diagram illustrating a possible phase separation in a CE capillary with BGEs containing less than 50% (v/v) acetonitrile with the phase separation between an acetonitrile-rich phase (ARP) near the inner capillary surface (containing a BGE zone with ion specie having higher pK_a values) and water-rich phase (WRP) in the central lumen layer of the capillary (containing a BGE zone with ion specie having lower pK_a values).

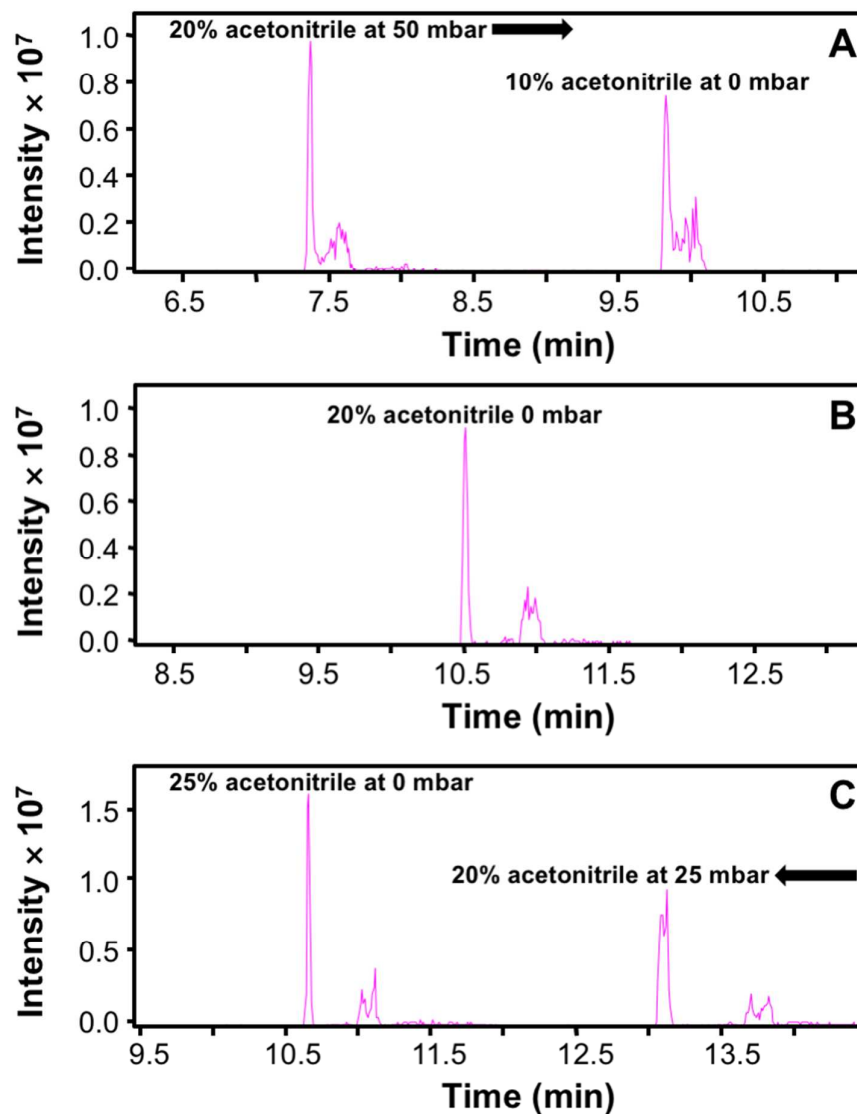


Figure S2. The overlay extracted mass spectrograms for peptide 2 at $m/z = 380.1$ as part of a mixture of five peptides dissolved in a solution containing 20% (v/v) acetonitrile in a mixture of HCOONH_4 buffer, pH 2.98 and HCOONH_4 buffer, pH 6.80, mixed in a ratio of 1 : 10 to generate a second eigenpeak, and run under the same condition as described in the legend to Figure 2.1. The result was achieved with different percentages of acetonitrile in 20 mM HCOONH_4 , pH 6.80 running buffer with the application of different pressures as indicated, (A) 20% (v/v) acetonitrile with 50 mbar additional pressure applied or 10% (v/v) acetonitrile with no additional pressure applied (0 mbar) in the same direction as the EOF, (B) 20% (v/v) acetonitrile with no additional pressure applied (0 mbar) in either direction, and (C) 25% (v/v) acetonitrile with no additional pressure applied (0 mbar) or 20% (v/v) acetonitrile with 20 mbar additional pressure applied in the direction opposite to the EOF.